ISSN (Print) 1226-1750
ISSN (Online) 2233-6656
Journal of Magnetics 20(3), 221-228 (2015) http://dx.doi.org/10.4283/JMAG.2015.20.3.221

Microstructure and Magnetic State of Fe_3O_4-SiO_2 Colloidal Particles

P. V. Kharitonskii[1], K. G. Gareev[1]*, S. A. Ionin[1], V. A. Ryzhov[2], Yu. V. Bogachev[1], B. D. Klimenkov[1], I. E. Kononova[1], and V. A. Moshnikov[1,3]

[1]Saint Petersburg Electrotechnical University "LETI", 197376, 5th Prof. Popova Str., Saint-Petersburg, Russia
[2]Petersburg Nuclear Physics Institute Named by B.P. Konstantinov, National Research Centre "Kurchatov Institute", 188300, Orlova Roscha, Gatchina, Leningrad District, Russia
[3]Saint Petersburg Polytechnic University, 195251, 29th Polytechnicheskaya Str., Saint-Petersburg, Russia

(Received 2 May 2015, Received in final form 21 August 2015, Accepted 24 August 2015)

Colloidal particles consisted of individual nanosized magnetite grains on the surface of the silica cores were obtained by two-stage sol-gel technique. Size distribution and microstructure of the particles were analyzed using atomic force microscopy, X-ray diffraction and Nitrogen thermal desorption. Magnetic properties of the particles were studied by the method of the longitudinal nonlinear response. It has been shown that nanoparticles of magnetite have a size corresponding to a superparamagnetic state but exhibit hysteresis properties. The phenomenon was explained using the magnetostatic interaction model based on the hypothesis of iron oxide particles cluster aggregation on the silica surface.

Keywords : magnetite, silica, colloidal particles, superparamagnetism, longitudinal nonlinear response, magnetostatic interaction

1. Introduction

Magnetite nanoparticles have attracted a great deal of attention because of their unique physicochemical properties and great potential use in various biomedical applications, such as contrast agents in magnetic resonance imaging (MRI), carriers for targeted drug delivery, radio frequency hyperthermia, the magnetic separation in microbiology, biochemical sensing [1-4], etc.

Magnetic colloidal particles based on iron oxide in a biologically inert and stable coating of silica can be used as an embolic material for catheter embolization of blood vessels under control of the magnetic resonance angiography. This approach is a prospective replacement of the traditional X-ray computed angiography with radioactive intravenous contrast agents. The use of iron oxide nanoparticles as the agents for the radio frequency arterial embolization hyperthermia is described in the papers [5, 6]. Modified commercial embolic materials based on chitosan [7] and gelatin [8] with iron oxide nanoparticles enhancing MRI contrast are tested.

*Corresponding author: Tel: +7-812-234-31-64
Fax: +7-812-234-31-64, e-mail: kggareev@yandex.ru

However, the magnetite nanoparticles are unstable in air and easily agglomerated after synthesis. The surface coatings and functionalization or formation of composite samples with nanoparticles on surface and in pores of some chemically stable material like silica could effectively solve these problems [9-13].

When the distance between magnetic nanoparticles (NPs) in colloidal solution is large enough, one can neglect by NP interactions. The magnetic behavior of an assembly of non-interacting fine particles (~10 nm in our case) in single domain state with uniaxial anisotropy is understood on the basis of Neel's arguments [14] that led to the concept of superparamagnetism (SPM) and blocking temperature T_b [15]. In this simple case a magnetic moment of NP is aligned along this axis and without an external magnetic field both directions of magnetization along the anisotropy axis are equivalent, while at presence of field one of them is preferred. After the field switching off, magnetization of an ensemble of non-interacting NPs should mount the energy barrier $E_b = KV$ to rotate back to the state defined by anisotropy, which takes a time. Here K is a constant of effective anisotropy, which includes magnetocrystalline, shape and surface anisotropies, and V is a volume of particle. The relaxation time of this process τ is given by $1/\tau = \Gamma = f_0 \exp(-E_b/kT)$

[16, 17], where the Larmor frequency f_0 is of the order of 10^9 s^{-1}. Because the particle volume V and temperature T are both in the exponent, the value of τ is strongly dependent on them. The probability that the magnetization remains in its original position during time t after switching off the external field can be written as $P(t) = \exp(-t/\tau)$, that gives for retentivity $M_{ret}(t)/M_0 = \exp(-t/\tau)$. Thus, if the registration time t is less than τ, the M_{ret} will be detected. For standard measurements of M_{ret} the time $t^* = 100$ s is normally used that gives the limit of SPM behavior $KV = 25kT$. From this relation for the ensemble of identical particles the blocking temperature T_b is introduced, above which the behavior of the system will be superparamagnetic without the field hysteresis in $M(H)$. It is given by expression $T_b = KV/25k$ [16, 17].

In experiments an increase of the blocking temperature with particle density has been reported and attributed to dipolar interactions between the particles [18-24]. In contrast to these findings, Mørup and Tronc [25] observed a decrease of the blocking temperature with particle density. Furthermore, the remanence of fine particle assemblies is usually found to decrease due to dipolar interactions [19, 20, 24], while increasing values with particle concentration have been reported [26]. Finally, hysteresis measurements showed a decrease of the coercivity with particle density and again this behavior was attributed to dipolar effects [19, 20].

As it was stated in work [27], composite nanoparticles consisted of iron oxide and silica form stable aqueous solution when it is not influenced by external magnetic field. Synthesis of the colloids was provided by R. Massart reaction [28] in highly dispersed silica solution obtained by sol-gel process. Spin-spin nuclear magnetic moments relaxation times were estimated by nuclear magnetic resonance relaxometry. It was found that constant external magnetic field leads to intensification of aggregation and sedimentation processes and thus elongates spin-spin relaxation times.

In this work authors continued earlier study of sol-gel method derived colloids based on iron oxide coated silica. As it was stated on work [29] obtained magnetic particles form chain aggregates under the influence of constant magnetic field. Absence of outer coating provokes intensive oxidation of magnetite and its transition to maghemite and hematite [30]. It is planned to modify described synthesis technique to achieve more chemical and aggregative stability of the colloid.

There were two principal tasks in present work. The first one was to confirm an origination of magnetic nanoparticles (MNs) on surface and in pores of SiO_2 and clarify whether they are in a single domain state. Since they should reveal strong nonlinearity, to investigate their magnetism we employed very sensitive method of nonlinear longitudinal response (NLR) to a weak ac magnetic field in parallel to it steady field [31]. In this case, a generation of the second harmonic of magnetization was recorded as a function of steady field at different temperatures. The second task was to estimate whether NP's interactions had an effect on their magnetic response at studied concentration of NPs. The method provides information both on static and dynamic magnetic properties, which is rather complete magnetic characterization of the material.

2. Experimental Methods

Synthesis of colloidal particles was obtained by two-stage technique described in papers [27] and [32]. Tetraethoxysilane (TEOS) isopropanol-based sols were gelated by adding ammonia aqueous solution. After drying and thermal treatment at 300ºC the resulting powder was dispersed using the 100 W ultrasonic generator in an aqueous iron-II sulphate and ferric chloride-III taken in the molar ratio 1:2 respectively. Then ammonia aqueous solution was added and large particles fraction was separated after settling the solution for 24 hours.

The microstructure of silica powders were studied by thermal desorption of nitrogen using device SORBI (JSC "META"). Calculation of the specific surface area was based on the BET theory of multilayer adsorption. Neglecting porosity the average particle size can be estimated on the basis of measurements of the specific surface area [33]:

$$D = \frac{6}{SSA\rho}, \tag{1}$$

where $\rho = 2{,}65$ g/cm^3 – silica true density.

To study shape and size of particles by atomic force microscopy in tapping scanning mode scanning probe microscope NTEGRA-THERMA (JSC "NT-MDT") was applied. Determination of crystalline phases was carried out using a desktop X-ray diffractometer "Farad" ("Expertcentre"), equipped with chrome cathode, $\lambda_{Cr\text{-}K\alpha 2} = 0.2291$ nm. The size of the crystallites was estimated by the equation of Debye-Scherrer as in [34]:

$$d = \frac{0.97\lambda}{\beta\cos\theta}, \tag{2}$$

where $\lambda = 0.2291$ nm, a $\beta = 0.5B - b + \sqrt{B(B-b)}$, B – the total width of the line, b - width of reference lines in the corundum etalon diffraction pattern at the same angle range.

Investigation of magnetic state of composites under study was performed by measurements of nonlinear response to a weak ac field. The second harmonic of magnetization, M_2, of the longitudinal nonlinear response (NLR) was measured in the parallel steady and alternating magnetic fields $H(t) = H + h\sin\omega t$ (h = 13.8 or 19.5 Oe, $f = \omega/2\pi \approx 15.7$ MHz) under condition $M_2 \propto h^2$. The last allows one to analyze the results in the framework of perturbation theory. ReM_2 and ImM_2 phase components of M_2 response were simultaneously recorded as the functions of H at the various sample temperatures in the range from 190 K up to 295 K provided by cryostat with nitrogen flow. The steady field H was slowly scanned symmetrically relative to the point $H = 0$ with frequency F_{sc} for control of a field hysteresis in the signal, which appearance due to symmetry properties of M_2 indicates the presence of a spontaneous ferromagnetic moment in a sample. The method is very sensitive to an appearance of a ferromagnetic (FM) component in magnetization owing to its large nonlinearity in weak magnetic fields. The amplitude of H-scan was 300 Oe and F_{sc} could be changed over the range 0.01-10 Hz. An installation and a method of separation of the M_2-phase components have been described previously [31]. The sensitivity of the measurements above was ~10^{-9} emu.

3. Experimental Results

As it was stated in work [35] with the decrease of iron oxide fraction in the composite (composites with the content of 90, 70, 50, and 30 mol.% $FeCl_3 \cdot 6H_2O$ in the initial solution were considered) the intensity of reflexes in X-ray diffraction pattern decreases with respect to the background with approximate invariance of their width, which could be explained by the increase of the fraction of the X-ray amorphous silica phase. Thus, to estimate the grain size the specimen of 80 mol. % $FeCl_3 \cdot 6H_2O$ in the initial solution was used in work [35]. So in this paper the specimen derived from the initial sol of 30 vol.% TEOS (further Fe_3O_4-30%TEOS) was taken. The X-ray diffraction pattern of powder Fe_3O_4-30%TEOS shown in Fig. 1 could be indexed with the Fe_3O_4 single phase. Finding the width of the peak at 2θ = 53.6º B(53.6º) = 0.015 rad from this diffractogram, and using the known width value of reference line in the corundum etalon b(53º) = 0.0027 rad, in accordance with the formula (2) we obtain the average grain size of magnetite NPs $d \approx 8$ nm. The found width of considered reflection is just between the width of corresponding peaks in diffraction patterns obtained from samples, consisting of Fe_3O_4 NPs with average particle size 5 and 10 nm [36]. This confirms the correctness of our finding. Thus, one can wait superparamagnetic behavior with zero coercive force H_c of our samples in case noninteracting magnetite grains with close to spherical form [16, 17].

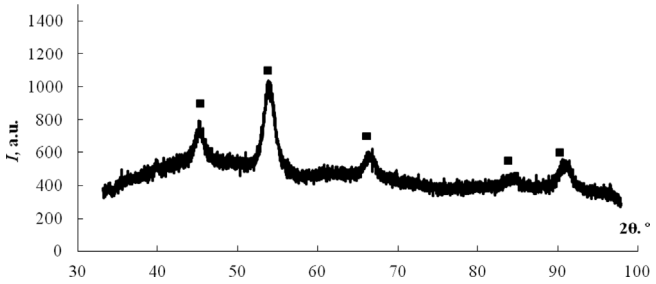

Fig. 1. XRD pattern of the dried precipitate the Fe_3O_4-30%TEOS sample.

Fig. 2 shows the experimental specific surface area on TEOS content in the initial sol dependence. As noted in [32], the highest efficiency of spin-spin relaxation of the protons magnetization can be achieved by using colloidal nanoparticles derived from sol with 60 vol.% TEOS which correlates with the maximum of the specific surface area about 60…70 vol.% TEOS content. So specimens based on initial sol with 60…70 vol.% TEOS were used for further investigations.

To estimate the size of silica particles the results of specific surface area measurement shown in Fig. 2 and the formula (1) can be used. Then the powder SiO_2 based on the initial sol containing 30 vol.% TEOS has an average diameter $\langle D \rangle \approx 80$ nm, while the sample on the basis of 70 vol.% TEOS sol consists of particles with $\langle D \rangle \approx 20$ nm. This estimation is not consistent with the result obtained by analysis of AFM-image of layer deposited from a suspension of silica particles. As seen in Fig. 3b, the average size found from treatment of AFM-image of the latter sample is $\langle D \rangle \approx 100$ nm. The dis-

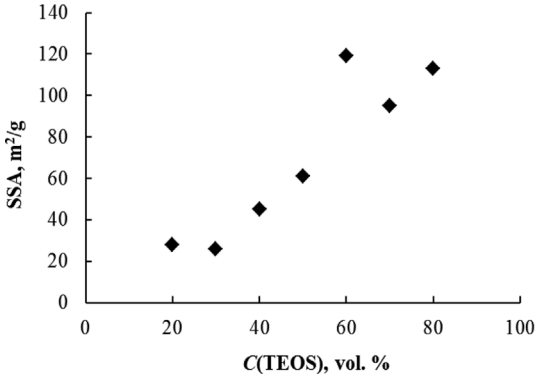

Fig. 2. Dependence of specific surface area on the volume content of the TEOS in the initial sol.

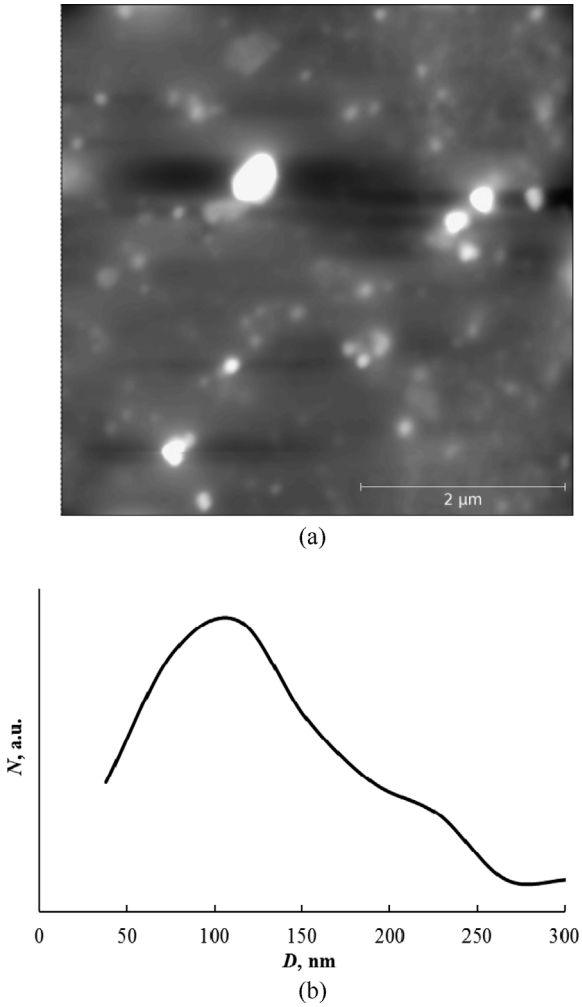

Fig. 3. AFM image (a) and particle size distribution in the layer deposited from the Fe_3O_4-70%TEOS sample (b).

crepancy can be explained by the presence of indistinguishable by AFM micropores on the surface of silica particles, which increases specific surface area, in accordance with the results of [34]. If the pore sizes are 5…10 nm it is possible to assume its role as a limiting factor for the growth of magnetite crystallites.

Above the Verwey temperature, T_V ~120 K, magnetite has a cubic spinel structure (space group $Fd3m$), with lattice parameter a_0 ~ 8.397 E and the O atoms arranged in a face-centered-cubic (fcc) lattice. The lattice can accommodate Fe^{3+} on the tetrahedral site (A) and Fe^{3+} and Fe^{2+} on the octahedral site (B) in antiparallel arrangement, yielding ferrimagnetic order below T_C ~ 850 K. Bulk magnetite has cubic magnetic anisotropy, with the <1 1 1> and <1 0 0> directions being the easy and hard axes of magnetization, respectively. At room temperature, the first-order magnetocrystalline anisotropy constant has a negative value ($K_1 = -1.35 \times 10^5$ erg/cm^3) [37]. Application of a simple model with uniaxial effective anisotropy K for analysis of ensemble of Fe_3O_4 NPs with a close to spherical form behavior leads to effective value $K \approx K_1/12 \sim 1.1 \times 10^4$ erg/cm [36]. The spherical form of NPs provides to a reduction of surface anisotropy contribution to effective anisotropy [38].

Let us go to magnetic data obtained by measurements of second harmonic generation under a weak linear polarized ac magnetic field (fundamental frequency f = 15.7 MHz) in the presence of parallel to it slowly scanned steady field H. Magnetization M of an ensemble of magnetic NPs is characterized by large nonlinearity in a weak magnetic field due to large magnetic moment of an individual particle ~10^3–10^4 μ_B [16]. This leads to a presence of characteristic signals with extremes in a weak field H in both phase components Re$M_2(H)$, Im$M_2(H)$ of second harmonic of magnetization M_2 recorded versus H [39]. We suppose the model of uniaxial magnetic anisotropy is applicable to NPs under consideration. Under condition $M_2 \propto h^2$ perturbation theory gives that main contribution to Re$M_2(H) \propto \partial^2 M(H)/\partial H^2$ is due to a nonlinearity of magnetization curve $M(H)$, whereas the main reason for Im$M_2(H)$ origination is owing to an effect of external field on process of magnetic relaxation because the presence of $H(t)$ modifies the energy barrier between two orientation of NP's magnetic moment along anisotropy axis. This contribution is proportional to $(\partial\Gamma(H)/\partial H)\cdot(\partial M(H)/\partial H)$ [39]. In our case of the periodic H-scan and synchronous detection of a response, H-hysteresis will be observed in M_2(H) response of single domain NP ensemble, if a period of H-scan $1/F_{sc} \le \tau = 1/\Gamma$. Therefore, in blocking regime below T_b the field hysteresis should depend on F_{sc} [39]. We characterize further the field hysteresis in the second harmonic of magnetization by a value of "coercive force" H_{C2} in Re$M_2(H) \propto \partial^2 M(H)/\partial H^2$ determined from the condition Re$M_2(H_{C2} = 0)$ and associated with coercive force H_C in magnetization $M(H)$. To clarify whether magnetite NPs in single domain state originate really in our composite sample we studied the $M_2(H)$-response dependences on T and F_{sc}. Fig. 4 presents the phase components Re$M_2(H)$ and Im$M_2(H)$ recorded versus H for colloidal solution of the sample, derived on the basis of sol with 60 volume percents of TEOS, at F_{sc} = 8 Hz, amplitude of *ac* field h = 19.5 Oe and T = 286 K. The signals reveal extremes in a weak H in the both phase components, and exhibit field hysteresis. Note, the sign of signal in ImM_2 (positive in region $H > 0$) is opposite to that in ReM_2 (negative in region $H > 0$) in accordance with our expectations. These peculiarities of $M_2(H)$ response confirm the origination of magnetic NPs in our composite. As can be seen from the Fig. 4 the field

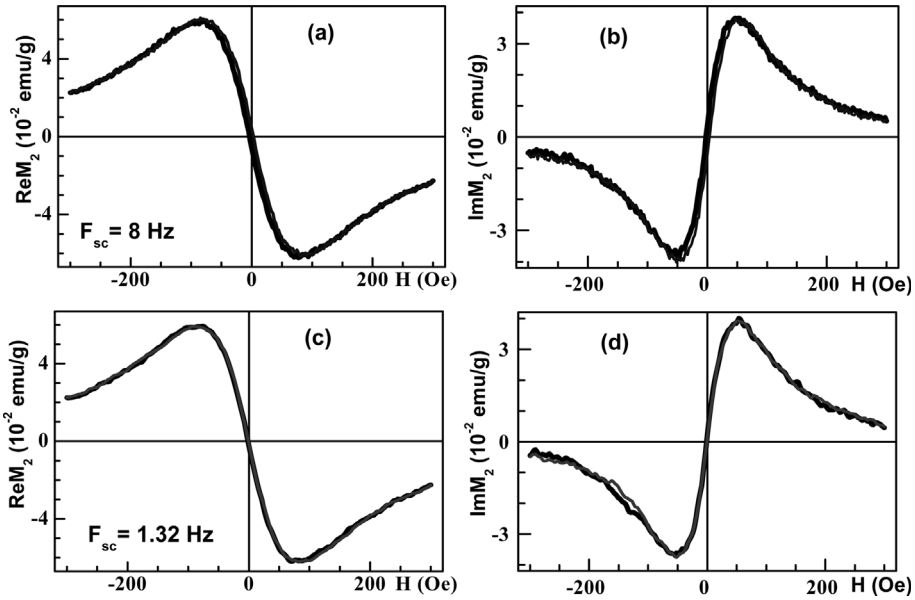

Fig. 4. Phase components ReM_2 and ImM_2 of second harmonic of magnetization vs H at different F_{sc} for the sample Fe_3O_4-60%TEOS at T = 286 K, h = 19.5 Oe. Panels (a), (b) present the response registered at F_{sc} = 8 Hz, while panels (c), (d) do this for F_{sc} = 1.32 Hz.

hysteresis is rather weak at F_{sc} = 8 Hz and practically disappears at F_{sc} = 1.32 Hz, when a time measurement is $t^* \approx 1$ s. We shall further characterized the latter by a value of H_{C2} that is determined from the condition $ReM_2(H_{C2}) = 0$, which is like to coercive force in $M(H)$ but can differs by the value, whereas hysteretic behavior of Im$M_2(H)$ can be more complex.

Fig. 5 displays the dependence of H_{C2} on frequency of H-scan found for the colloidal solution of Fe_3O_4-60%TEOS sample at T = 294 K and h = 13.8 Oe. As it is seen from the Figure, the hysteretic behavior at $T \sim 294$ K disappears with decreasing F_{sc} in agreement with Fig. 4. This behavior suggests single domain state of NPs.

Let us go to effect of temperature on hysteretic properties of ReM_2 response of colloidal solution of Fe_3O_4-60%TEOS sample. Fig. 6 shows H_{C2} dependence on temperature for values of F_{sc} = 8 and 1.3 Hz. Field hysteresis is practically disappeared below 240 K at $F_{sc} \leq 1.3$ Hz. Assuming $T_b \approx 240$ K we can estimate the constant of effective anisotropy. For the time of measurement $t^* \approx 1$ s (F_{sc} = 1.3 Hz) we have $T_b \approx KV/21k$, from which $KV \approx 21kT_b \approx 7 \times 10^{-13}$ erg for the average anisotropy energy of NP. Taking an average size of NP $d \sim 10$ nm we find the effective anisotropy constant $K \sim 1.4 \times 10^6$ erg/cm^3 that is much greater than even crystalline anisotropy of bulk Fe_3O_4. According to Goya *et al.* [36], only a weak field hysteresis was observed at T = 296 K in $M(H)$ dependence for Fe_3O_4 NPs of spherical form with average size $d \approx 10$ nm. Found by us a weak hysteretic behavior

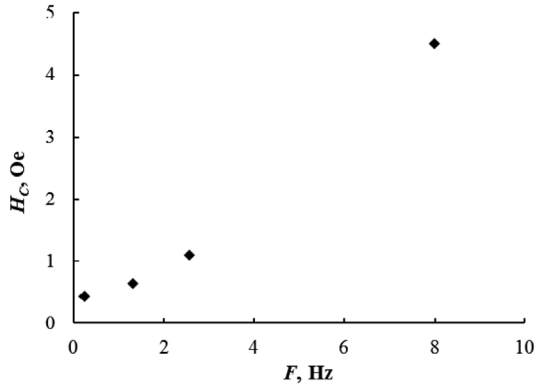

Fig. 5. Dependence of "coercive force" H_{C2} of Re$M_2(H)$, found from the condition $ReM_2(H_{C2}) = 0$, on frequency of steady field scan F_{sc} obtained for the sample Fe_3O_4-60%TEOS at T = 294 K and h = 13.8 Oe.

of $M_2(H)$ response at T = 294 K (see Fig. 5) in Fe_3O_4-60%TEOS sample with close estimation of average size of Fe_3O_4 grains $d \approx 8$ nm (see above), suggest the close to spherical form of the latter. This implies that found in our sample large effective anisotropy constant $K \sim 1.4 \times 10^6$ erg/cm^3 > K_1 of bulk Fe_3O_4 is due to NP dipolar interactions, which affect their magnetic characteristics.

4. Theoretical Model and Discussion

In an ensemble of non-interacting magnetic particles the regime of its magnetization behavior at some temperature

T depends on its value relative to blocking temperature T_b, as discussed above. The latter is determined by a size of a particle and magnetic anisotropy and necessary for providing of blocking regime volume of particle can be written as [14-16]:

$$v_b = \frac{2kT_b}{M_s(T_b)H_0(T_b)} \cdot \ln(tf_0), \tag{3}$$

where $M_s(T_b)$ и $H_0(T_b)$ – saturation magnetization and critical field (in our case it is the field of anisotropy $H_A(T_b)$) of single-domain particle respectively at the blocking temperature T_b; t – measurement time, f_0 – frequency factor. The estimation of the average blocking volume for Fe_3O_4 NPs in our sample from this expression, using found above T_b = 240 K and estimation for constant of effective uniaxial anisotropy $K \approx 1.6 \times 10^6$ erg/cm^3 (we take $H_A = 2K/M_S$ [16], $f_0 = 10^9$ Hz and t = 1 s, see above), gives $v_b \approx 4.3 \times 10^{-19}$ cm^3. Suggesting the spherical form of the NPs (see argumentation above) we found the estimation of average diameter of the NPs, $d_b \approx$ 20 nm, which is larger of the value found from the X-ray data (8 nm). This suggests that approximation of non-interacting NPs is incorrect for our samples. Indeed, in our case of magnetite grains placed on surface and in pores of the porous silica particles, these grains may be combined in clusters (probably inside and around the pores, which may be considered as preferable sites for NP's formation and binding with SiO_2 surface) with a sufficiently high concentration, in which the energy of their dipole-dipole interactions can be comparable with thermal fluctuations. These interactions will provide the preferable parallel orientation of particle magnetic moments and some its stabilization with respect to thermal fluctuations. Thus, the magnetization of the ensemble of colloidal single domain magnetic particles can reveal time dependent remanent magnetization and field hysteresis with $H_C \neq 0$ above the blocking temperature of individual particle.

Let us consider a system of weakly interacting single-domain magnetic particles, exhibiting uniaxial anisotropy, with the same critical fields, under external field **H**. The energy of the magnetic moment of the particle is known [40]:

$$E = -\frac{1}{2}mH_0\cos^2\theta - (\mathbf{m}, \mathbf{H}+\mathbf{H}_i), \tag{4}$$

where θ is the angle between the easy axis and the particle magnetic moment $\mathbf{m} = v\mathbf{M}_s$. The magnetic moments of particles are oriented along magnetic anisotropy and magnetic field $\mathbf{H} + \mathbf{H}_i$, the random interaction field $\mathbf{H}_i$ being collinear to **H**. If **m** is parallel to **H** ($\theta = 0$ – first state), the energy of particle is

$$\Delta E_1 = \begin{cases} \dfrac{m(H_0 + |\mathbf{H}+\mathbf{H}_i|)^2}{2H_0}, & |\mathbf{H}+\mathbf{H}_i| \le H_0, \\ 2m|\mathbf{H}+\mathbf{H}_i|, & |\mathbf{H}+\mathbf{H}_i| > H_0. \end{cases} \tag{5}$$

At the second state ($\theta = \pi$)

$$\Delta E_2 = \begin{cases} \dfrac{m(H_0 - |\mathbf{H}+\mathbf{H}_i|)^2}{2H_0}, & |\mathbf{H}+\mathbf{H}_i| \le H_0, \\ 0, & |\mathbf{H}+\mathbf{H}_i| > H_0. \end{cases} \tag{6}$$

The thermal fluctuations induce transitions of particle magnetic moment between these two states and the probabilities of transition are:

$$P_1(0,\pi) = f_0 \exp[-\Delta E_1/(kT)],$$
$$P_2(\pi,0) = f_0 \exp[-\Delta E_2/(kT)], \tag{7}$$

while "life times" of magnetic moment at each state equal $\tau_1 = P_1^{-1}$ и $\tau_2 = P_2^{-1}$. Obviously, $\tau_1 > \tau_2$, and ratio $\tau_1/\tau_2 = \exp[2m|\mathbf{H}+\mathbf{H}_i|/(kT)]$ grows exponentially with increase of the grain volume. Therefore, if the particle magnetic moments are considered as blocked at $\tau_1 >$ measurement time t, we obtain the dependence of the necessary particle volume for transition to blocking regime (blocking volume) on the interaction field H_i [40]:

$$v_b(H_i) = \begin{cases} v_b/\left(1 + \dfrac{|H+H_i|}{H_0}\right)^2, & |H+H_i| \le H_0, \\ v_b/\left(1 + \dfrac{4|H+H_i|}{H_0}\right), & |H+H_i| > H_0. \end{cases} \tag{8}$$

Here H is the external magnetic field and the magnetostatic interaction random field H_i is collinear to H for the cluster. Thus, the magnetostatic interaction can significantly reduce the blocking volume, especially at low coercive particles. Hence, the magnetization of the cluster will be determined by the grains, for which $v > v_b(H_i)$.

The coercive force H_C is determined in accordance with the formula

$$H_C = H_0 - [2kTH_0 \ln(tf_0)/v_bM_S]^{1/2}. \tag{9}$$

The coercive force H_C becomes equal to H_0 only at T = 0 K, and with increasing of temperature H_C drops to zero at the transition from blocking regime to the superparamagnetic one. When the independent parameter is the particle diameter d, the ratio can be written as

$$H_C = H_0[1 - (d_b/d)]^{3/2}, \tag{10}$$

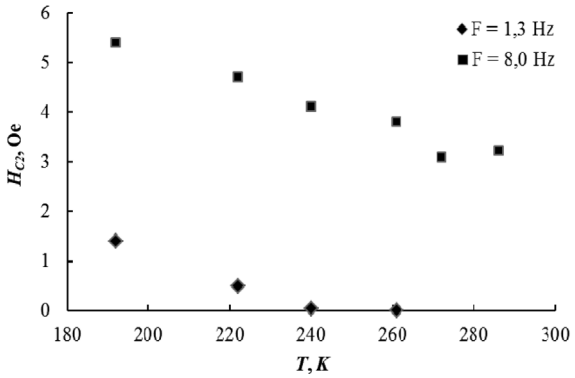

Fig. 6. Temperature dependence of "coercive force" H_{C2} in $\mathrm{Re}M_2(H)$, found from the condition $\mathrm{Re}M_2(H_{C2}) = 0$, obtained for the sample Fe_3O_4-60%TEOS at $h = 13.8$ Oe and frequency of steady field scan $F_{sc} = 1.3$ and 8 Hz.

where $d_b \sim [v_b(H_i)]^{1/3}$ is blocking diameter depending on random magnetostatic interaction field H_i.

Take a random field of magnetostatic interaction equal to the mean square field $\sigma = [M(H_i - \langle H_i \rangle)^2]^{1/2} \sim 1.3\eta^{1/2}M_s$, where $\eta \sim 0.2$ is volume concentration of magnetite particles in the cluster [40]. Then, calculation according to the formulas (8) and (10) for the spherical magnetite particles at room temperature gives the blocking diameter $d_b \sim 10$ nm. This explains the presence of field hysteresis $M_2(H)$ response at $T = 294$ K (Fig. 5) and agrees well with the result for average size of Fe_3O_4 nanoparticles (~ 8 nm) obtained above from the experimental data using the formula (2). As the temperature decreases from 286 K to 192 K magnetite magnetic parameters change slightly. According to expression (9) the coercivity should increase with decreasing temperature that corresponds to experimental data as well (see Fig. 6).

5. Conclusion

Structural and magnetostatic properties of composite colloidal particles Fe_3O_4-SiO_2 were studied by different experimental techniques and analyzed theoretically. Specific features of synthesized specimens, including two-level grain size hierarchy of about 100 and 10 nm, constrain authors to apply indirect methods of investigation. Size distribution of silica core was estimated by AFM and nitrogen thermal desorption techniques. Average size of iron oxide particles ($d \approx 8$ nm), covering the silica core, was calculated from XRD pattern using Debye equation.

The data on second harmonic generation under parallel *dc* and *ac* magnetic fields indicate single domain state of magnetite grains in our sample and allow us to find the blocking temperature $T_b \approx 240$ K. From the latter the estimation of constant of effective uniaxial anisotropy is obtained, followed by estimation of the blocking diameter of the Fe_3O_4 NPs, $d \sim 20$ nm. The discrepancy between measured average size of NPs and the estimation was overcame by taken into account non-random their distribution on a surface of the silica cores due to a presence of pores assumed from comparison of the specific surface area for SiO_2 particles and AFM data. It was suggested the pores create preferable sites for formation and binding the NPs that is accompanied by formation of grain clusters. The model taking into account the magnetostatic interactions of the Fe_3O_4 grains were used and described the reduction of their blocking diameter.

Acknowledgment

This work was partially supported by RFBR grant No. 14-03-31534.

References

[1] C. Sun, J. S. H. Lee, and M. Q. Zhang, Advanced Drug Delivery Reviews **60**, 1252 (2008).
[2] A. K. Gupta and M. Gupta, Biomaterials **26**, 3995 (2005).
[3] R. Olsvik, T. Popovic, E. Skjerve, K. S. Cudjoe, E. Hornes, J. Ugelstad, and M. Uhlen, Clinical Microbiology Reviews **7**, 43 (1994).
[4] M. N. Widjojoatmodjo, A. C. Fluit, R. Torensma, and J. Verhoef, Journal of Immunological Methods **165**, 11 (1993).
[5] N. Kawai, D. Kobayashi, T. Yasui, Y. Umemoto, K. Mizuno, A. Okada, K. Tozawa, T. Kobayashi, and K. Kohri, Vascular Cell **6**, 15 (2014).
[6] I. S. Smolkova, N. E. Kazantseva, K. N. Makoveckaya, P. Smolka, P. Saha, and A. M. Granov, Materials Science and Engineering C **48**, 632-641 (2015).
[7] S. Y. Choi, B. K. Kwak, H. J. Shim, J. Lee, S. U. Hong, and K. A. Kim, Diagnostic and Interventional Radiology **21**, 47 (2015).
[8] K.-H. Lee, E. Liapi, J. A. Vossen, M. Buijs, V. P. Ventura, C. Georgiades, K. Hong, I. Kamel, M. S. Torbenson, and J.-F. H. Geschwind, J. Vasc. Interv. Radiol. **19**, 1490 (2008).
[9] S. Y. Gan and M. Chow, Journal of Materials Chemistry **14**, 2781 (2004).
[10] A. Kaushik, R. Khan, P. R. Solanki, P. Pandey, J. Alam, S. Ahmad, and B. D. Malhotra, Biosensors and Bioelectronics **24**, 676 (2008).
[11] J. Sun, S. B. Zhou, P. Hou, Y. Yang, J. Weng, X. H. Li, and M. Y. Li, Journal of Biomedical Materials Research **80A**, 333 (2006).
[12] M. D. Butterworth, L. Illum, and S. S. Davis, Colloids

and Surfaces A: Physicochemical and Engineering Aspects **179**, 93 (2001).
[13] Q. Xu, X. J. Bian, L. L. Li, X. Y. Hu, M. Sun, D. Chen, and Y. Wang, Electrochemistry Communications **10**, 995 (2008).
[14] L. Neel and C. R. Hebd, Seances Acad. Sci. **228**, 664 (1949); Ann. Geophys. (C.N.R.S.) **5**, 99 (1949).
[15] C. P. Bean and J. D. Livingston, J. Appl. Phys. **30**, 120 (1959).
[16] B. D. Gullity and C. D. Graham, Introduction to Magnetic Materials, IEEE Press, WILEY (2009) p. 383.
[17] S. Bedanta and W. Kleemann, J. Phys. D: Appl. Phys. **42**, 013001 (2009).
[18] J. L. Dormann, L. Bessais, and D. Fiorani, J. Phys. C **21**, 2015 (1988).
[19] S. Gangopadhyay, G. C. Hadjipanayis, C. M. Sorensen, and K. J. Klabunde, IEEE Trans. Magn. **29**, 2619 (1993).
[20] R. W. Chantrell, In: Magnetic Hysteresis in Novel Magnetic Materials, by ed. G. C. Hadjipanayis, NATO Advanced Study Institute, Series E: Applied Sciences, vol. 338, Kluwer, Dordrecht (1997) p. 21.
[21] R. W. Chantrell, M. El-Hilo, and K. O'Grady, IEEE Trans. Magn. **27**, 3570 (1991).
[22] M. El-Hilo, K. O'Grady, and R. W. Chantrell, J. Magn. Magn. Mater. **114**, 295 (1992).
[23] K. O'Grady, M El-Hilo, and R. W. Chantrell, IEEE Trans. Magn. **29**, 2608 (1993).
[24] W. Luo, S. R. Nagel, T. F. Rosenbaum, and R. E. Rosensweig, Phys. Rev. Lett. **67**, 2721 (1991).
[25] S. Mørup and E. Tronc, Phys. Rev. Lett. **72**, 3278 (1994).
[26] S. Mørup, F. Bodker, P. V. Hendriksen, and S. Linderoth, Phys. Rev. B **52**, 287 (1995).
[27] Yu. V. Bogachev, K. G. Gareev, L. B. Matyushkin, V. A. Moshnokov, and A. N. Naumova, Phys. of the Sol. St. **55**, 2313 (2013).
[28] R. Massart. IEEE Trans. Magn. **17**, 1247 (1981).
[29] I. E. Kononova, K. G. Gareev, V. A. Moshnikov, V. I. Al'myashev, and O. V. Kucherova, Inorganic Materials **50**, 68 (2014).
[30] V. I. Al'myashev, K. G. Gareev, S. A. Ionin, V. S. Levitskii, V. A. Moshnikov, and E. I. Terukov, Physics of the Solid State **56**, 2155 (2014).
[31] V. A. Ryzhov, I. I. Larionov, and V. N. Fomichev. Zh. Tekh. Fiz. **66**, 183 (1996) [Tech. Phys. **41**, 620 (1996)]; V. A. Ryzhov, and E. I. Zavatskii, Patent No 2507525, registered in Russia 20.02.2014.
[32] Yu. V. Bogachev, Ju. S. Chernenco, K. G. Gareev, I. E. Kononova, L. B. Matyushkin, V. A. Moshnikov, and S. S. Nalimova, Appl. Magn. Reson. **45**, 329 (2014).
[33] D. Shaw. Introduction to Colloid and Surface Chemistry. Elsevier (1992) p. 320.
[34] I. E. Gracheva, G. Olchowik, K. G. Gareev, V. A. Moshnikov, V. V. Kuznetsov, and J. M. Olchowik, J. Phys. Chem. Sol. **74**, 656 (2013).
[35] I. E. Gracheva, V. A. Moshnikov, and K. G. Gareev, Glass Phys. Chem. **39**, 311 (2013).
[36] G. F. Goya, T. S. Berquo, F. C. Fonseca, and M. P. Morales, J. Appl. Phys. **94**, 3520 (2003).
[37] L. R. Bickford, J. M. Brownlow, and F. R. Penoyer, Proc. IEEE **104**, 238 (1957).
[38] F. Bodker, S. Mørup, and S. Linderoth, Phys. Rev. Lett. **72**, 282 (1994).
[39] V. A. Ryzhov, I. V. Pleshakov, A. A. Nechitailov, N. V. Glebova, E. N. Pyatyshev, A. V. Malkova, I. A. Kisilev, and V. V. Matveev, Appl. Magn. Reson. **46**, 339 (2014).
[40] P. V. Kharitonskii, A. M. Frolov, S. A. Boev, V. S. Rudnev, I. A. Tkachenko, V. P. Morozova, I. V. Lukiyanchuk, M. V. Adigamova, and A. Yu. Ustinov, Sol. St. Phen. **215**, 200 (2014).